City Research Online

City, University of London Institutional Repository

Citation: Faghih, F. & Ayoub, A. (2019). Mechanical and self-sensing properties of concrete reinforced with carbon nanofibres. Advances in Cement Research, 33(3), pp. 97-113. doi: 10.1680/jadcr.18.00209

This is the accepted version of the paper.

This version of the publication may differ from the final published version.

Permanent repository link: https://openaccess.city.ac.uk/id/eprint/23241/

Link to published version: https://doi.org/10.1680/jadcr.18.00209

Copyright: City Research Online aims to make research outputs of City, University of London available to a wider audience. Copyright and Moral Rights remain with the author(s) and/or copyright holders. URLs from City Research Online may be freely distributed and linked to.

Reuse: Copies of full items can be used for personal research or study, educational, or not-for-profit purposes without prior permission or charge. Provided that the authors, title and full bibliographic details are credited, a hyperlink and/or URL is given for the original metadata page and the content is not changed in any way.

City Research Online: http://openaccess.city.ac.uk/ publications@city.ac.uk

Mechanical and Self-Sensing Properties of Concrete Reinforced with Carbon NanoFibres

Faezeh Faghih[1] and Ashraf S. Ayoub[2]

[1] Doctoral Candidate, Dept. of Civil Engineering, City, University of London, London, UK

[2] Professor, Dept. of Civil Engineering, City, University of London, London, UK

Abstract

Concrete is extensively used in the construction industry; however formation and development of cracks undermines the integrity of the structure. Thus, both improving the mechanical properties of this material as well as efficient health monitoring of structures are essential tasks to be tackled.

The research covered in this paper is concerned with the effect of nano fibres on the mechanical properties of concrete. The use of nano fibres such as Carbon Nanofibre (CNF) within cementitious materials is found to be effective in enhancing the mechanical properties of concrete as well as its sensing ability. Most previous work focused on evaluating the micro-structure and mechanical behaviour of nano-reinforced mortar. Only a few studies attempted to evaluate the mechanical and sensing properties of nano-reinforced concrete with coarse aggregates.

The objective of this study is to fill this gap in the literature by evaluating the mechanical and self-sensing properties of Carbon Nanofibre concrete. Material tests were conducted on cylinders and beam samples of CNF concrete in order to develop the full compressive, tensile, and flexural constitutive behaviour including the post-peak response, as well as evaluate its self-sensing capability. The results obtained are valuable for analysis and design of large critical infrastructures employing CNF concrete.

Keywords: Nanostructure; Fibre reinforcement; Electrical properties; Testing; Carbon nanotube (CNT); Carbon nanofiber (CNF); Mechanical properties; Self-Sensing

Introduction

Different types of fibres are widely used to control cracking in fibre-reinforced concrete (FRC). The efficiency of these fibres is however dependant on their geometry and material properties, and they can be considered at multi-scale levels from nano to macro scale. Macro fibres (typically defined as fibres with diameters > 500 μm) can bridge macro cracks and improve post-peak toughness. Fine microfibers (typically defined as fibres with diameter < 50 μm) on the other hand, bridge the microcracks which delay the process by which the microcracks coalesce to form macrocracks. Nano-particles such as carbon nanotubes (CNTs) and carbon nanofibers (CNFs) exhibit unique properties with remarkable mechanical, physical and electrical properties and hence they have been gaining extensive scientific attention during the past years, and they are applied in many fields, including cementitious materials, to fabricate new materials with novelty functions.

CNT/CNF

The primary differences between the CNT and CNF are morphology, size, ease of processing, and price. Table 1 briefly compares the properties of the two fibres. Carbon Nanotubes (CNTs) are extremely small and their diameter is usually less than 20 nm with an elastic modulus of more than 1 TPa and an elastic strain capacity of 12%, which is 60 times higher than that of steel as discussed by Yazdanbaksh (2012) and Salvetat and Kuik (1997). Similarly, carbon nanofibers (CNF) are unique as they combine microscopic length (from 200 nm to 100 μm) with a nanoscopic diameter (1–200 nm), with greater strength to weight ratio than steel as noted by Sanchez and Ince (2009). Compared to CNTs, CNFs have a lower production cost (about 100 times lower) and are suitable for mass production.

The nano-reinforced cementitious composite could only benefit from the outstanding properties of the nanofibers when they are properly dispersed within the matrix. The difficulty in dispersing nanofibers in liquid media has been overcome using methods such as surface modification of fibres using surfactants in combination with sonication.

The dispersion and interfacial bond of CNF fibres and cementitious composite at CNF/cement weight ratio of 0.4% was investigated through experiments (Yazdanbakhsh et al. 2009, 2010). Two different

CNFs, as well as two different surfactants (non-ionic and polycarboxylate superplasticiser), were used. CNFs were dispersed in a water-surfactant solution and ultrasonically processed for 15 minutes. As the experimental results showed, the non-ionic surfactant was more effective in de-agglomeration of the CNFs in water. However, the addition of non-ionic surfactant was found incompatible with cement hydration to cement paste and it increased the amount of entrapped air remarkably. It was found that a polycarboxylate-based superplasticiser (i.e. weaker surfactant also known as water reducing admixture) could properly disperse a relatively high concentration (more than 1.0%) of CNFs in water.

Camacho-Ballesta et al. (2016) conduced the dispersion by mixing CNT and distilled water in a high-shear mixer for 10 min and afterwards an ultrasound treatment was applied for 5 min. They found 7.7% improvement in compressive strength of 0.25% CNT reinforced cement paste, while the flexural strength was improved by 19.4% when 0.5% fibre dosage was used. Tyson et al. (2011) conducted small-scale flexural tests on CNT and CNF reinforced cement paste. It was found that the addition of both CNT and CNF improved the peak displacement up to 150% (specimen with 0.2 wt% CNF) which is crucial for structural applications in which higher ductility and strain capacity is needed. In addition, the elastic modulus of cement paste was increased from 15 GPa to 24 GPa by addition of 0.2% CNF. Overall, the CNF fibres outperformed CNTs for displacement at failure, which was attributed to the higher aspect ratio of CNFs. In another study, Metaxa et al. (2013) investigated the mechanical performance and dispersion of CNF (0.048 wt%) reinforced cement paste. Initially, CNFs were added to a water/surfactant solution then subjected to an intensive sonication. It was concluded that the addition of CNF to cement paste offers a significant property enhancement to the cementitious nanocomposites, mainly increased flexural strength and stiffness, and crack control at the nanoscale. Yazdani and Mohanam (2014) studied the compressive strength and flexural strength of cement mortar reinforced with 0.1% and 0.2% of both CNT and CNF with water/cement ratios of 0.35-0.50. The mixing technique used was ultrasonication of fibres in water-surfactant mixture for 30 min and 15 min respectively for CNT and CNF. It was concluded that the best combination for compressive and flexural strength production was CNF composites (0.1%-0.2%) with w/c ratio of 0.35. Gao et al. (2009) investigated the mechanical properties of concrete and Self-Consolidating Concrete (SCC) containing

0.16%-2.5% CNF by volume of binder. The cylinder compressive strength of the concrete was increased by 42.7% for 0.16% CNF concentration. The authors believe that using SCC improved CNF dispersal and increased the electrical sensitivity of the concrete. Sivakumar (2011) used 0.5%, 1.0%, 1.5%, and 2.0% of CNF by volume of binder within SCC. CNF were mixed with water using a blender, and superplasticiser was then added. The characteristic compressive strength of the concrete increased by 29.4% for 1.0% CNF. Both flexural strength and split tensile strength increased with 0.5% and 1.0% then decreased for higher volume fractions. The maximum variation for the split tensile strength was as low as 0.6%. Another recent study on nanoconcrete was conducted by Meng and Khayat (2016) on mechanical properties of UHPC with carbon nanofiber. 0.5% micro steel fibre, 5% silica fume and 0-0.3% CNF were used. The compressive strength slightly increased by 5-8 MPa. The direct tensile strength and flexural strength was increased by 56% and 46% respectively for 0.3% CNF concrete and the energy absorption was increased by 108%. Gdoutos et al. (2016) conducted a fracture mechanics experiment study on MWCNT and CNF reinforced cement mortar prisms. In their study, CNF showed better performance than those MWCNT samples. The authors stated that besides good dispersion, the diameter, and the length of the CNF was responsible for the better performance. The addition of 0.1% wt. CNF to the mortar resulted in an increase of 105.9% in flexural strength and 94.3% in modulus of elasticity. Overall, the nano-reinforced mixes exhibited less brittle behaviour.

Howser et al. (2011) tested short shear critical columns built with 1% dosage of CNF reinforced self-consolidating concrete (SCCNFC) under reversed cyclic load. Steel fibre reinforced SCC (SCSFC) and SCC columns with no fibres (SCRC) were also tested for comparison purposes. A definite yielding of longitudinal steel occurred in both the SCRC and SCCNFC columns with visible compression strut, while steel fibre reinforced column failed with one dominant shear crack. This was attributed to the absence of transverse shear ties. The ultimate normalised capacity, deflection, and ductility of SCCNFC column was respectively 30.7%, 34.9%, and 35.1% higher than the SCRC column. It was concluded that the addition of carbon nanofibers to concrete increased the strength and ductility of the short column.

The effectiveness of silica fume in maintaining a good dispersion was also proposed and studied by researchers (Yazdanbaksh, 2012; Sanchez and Ince, 2009; Kim et al. 2014). This novel and effective method of using silica fume to immobilise and stabilise the nanofilaments already dispersed in cement paste prevent them from migrating towards each other. Kim et al. (2014) studied the SEM images of dispersed CNTs in the cement matrix and it was found that using silica fume strongly affected the mixing process of nanofibers, and they were dispersed individually hence increasing the compressive strength. The study by Sanchez and Ince (2009) on the effect of silica fume on the dispersion enhancement of the CNF in cement composite revealed that silica fume particles due to their small size disrupted the individual CNF fibre-fibre interaction that held them as clumps during the dry mixing. This resulted in an overall greater, though not complete, dispersion of the CNFs throughout the cement paste.

Another enhanced property upon the introduction of the carbon nanofibers to the matrix is increased electrical conductivity of the cementitious materials. This feature is explained in the following section.

Self-health monitoring

Since the birth of nanotechnology and development of cementitious materials, advanced methods have emerged for structural health monitoring, providing measurable electrical responses to applied strain. Incorporating conductive nanomaterials (such as carbon nanofiber, carbon fibre, or carbon black) within concrete, results in developing a material that can be conductive and piezoresistive (resistance changes with strain), which is so-called *smart concrete*. The self- sensing capability of the nanoconcrete is based on its piezoresistivity. Electrically conductive concrete allows performing resistivity measurements, which could be used to analyse the strain or stress variations in the structural member.

Researchers (Kim et al., 2014, Wen and Chung, 2001, Cao and Chung, 2001) found that adding silica fume is effective in lowering the electrical resistance of carbon fibre reinforced cement mortar, and it enhances the electromagnetic shielding effectiveness of CNT-CNF/cement composites causing the nanofibers to have noticeable impact on the electrical properties of the cement composites, and decreasing its electrical resistance.

Azhari and Banthia (2017) studied both carbon fibre and carbon nanotube as the conductive filler in cement paste. 10% improvement in conductivity was observed for the hybrid sensor (containing both carbon fibre at 15% and MWCNT at 1% by volume). Cylindrical samples showed nonlinear decrease in resistivity under linear compressive load. The electrical resistivity changed in a reversible manner, corresponding to the applied cyclic load, increasing with the increase in tensile strain and vice versa. The response of CNT-cement based material to both sinusoidal compression loads and axial loads with forward/backward sweep variation of the frequency was measured by Materazzi et al. (2013) to monitor their electrical response for measuring dynamically varying strain in concrete structures. Good correlation was qualitatively observed between axial strain and electrical resistance, and normalised input and output were almost perfectly overlapped. Thus, it was concluded that CNT-cement composites provide useful information for SHM to the dynamic range. Dalla et al. (2016) investigated the damage-sensing capability of CNT-cement mortar with 0.6 wt.% loading and CNF-cement mortar with 0.2 wt.% and 0.6 wt.% loading. Piezoresistive behaviour of both types of mortar was analysed and they showed fully recoverable electrical resistance varying in an inverse relation to applied compressive stress. Three-point bending test on small prismatic mortar samples showed that both fibres gave remarkable damage sensing capability to the mortar evidenced by dramatic resistivity jumps at maximum loading level, thus providing valuable warning sign. Camacho-Ballesta et al. (2016) also found that for MWCNT cement paste, the Fractional Change in Resistance (FRC) was well correlated with the stress applied to the specimen under compression. Also, sensitivity was enhanced when the current intensity was increased. The best performance as strain sensor was obtained for the 0.05% CNT composite, reaching values of gauge factor up to 240. The electrical conductivity of the hybrid specimens (0.2% CNF/0.2% CNT) was found significantly higher than single CNT or CNF cement composites by Noiseux-Lauze and Akhras (2013). The relationship between strain and resistivity was fairly linear and a gauge factor of approximately 70 was measured. In addition to the referred research, other researchers also found an improvement in the conductivity of CNT/CNF reinforced cementitious materials, and a relationship between strain and stress was found (Galao et al., 2014; Sasmal et al., 2017; Rhee and Roh, 2013).

Research Significance

The main inspiration for this research was to extend the study of nanofiber reinforced concrete by developing its full mechanical properties including the post-peak response, as well as evaluating its electrical and self-sensing properties. Previous research focused on investigating the behaviour of mortar specimens, and only a few studies attempted to evaluate the behaviour of concrete specimens, particularly their full mechanical behaviour under tensile and compressive loads. The research will therefore fill an important gap in the literature and is considered vital for assessing the performance of large critical infrastructures employing CNF concrete. Further, the strain-sensing capability of carbon nanofiber reinforced concrete (CNFRC) currently could be a major advantage in civil engineering whose main purpose is the early assessment of structural damage. Therefore, it is important to investigate the sensing properties of such materials, and feed the findings into the industry.

Experimental Programme

A total of five concrete mixtures, incorporating different contents of CNF, were produced in this set of experiments to evaluate the effect of carbon nanofibers on concrete. The Plain Concrete (PC) mixture was dealt as the control mixture with no fibres. CNFRC were produced incorporating 0.25%, 0.5%, 0.75%, and 1.0% CNF by binder volume. These samples are denoted as CNFRC0.25, CNFRC0.5, CNFRC0.75, and CNFRC1.0, which indicates the concrete type followed by the fibre percentage used for the mix. Three samples of beams and six cylinders were replicated in each test. Mechanical properties of the material under flexure, uniaxial compression, and split tensile forces were established. Also, self-health monitoring of the beam samples under flexure were studied for this group.

Constituent materials

For binder materials, Type I Portland cement, and dry undensified silica fume Grade 940U (Elkem Materials, Inc.) were used with bulk density of 200-350 kg/m^3 (Table 2). Silica fume acts physically as a filler and chemically as a highly reactive pozzolan. Sharp sand was used as fine aggregate and gravel with maximum size of 10mm was used as coarse aggregate.

Heat treated carbon nano fibre (Pyrograf-III, PR-19-XT-LHT) provided by Applied Sciences Inc. were used. The properties of these fibres are summarised in Table 3 (Pyrograph Products, 2013). These fibres are heat-treated to temperatures of 1500°C, which carbonizes chemically vapour deposited carbon present on the surface of the fibre to a short range ordered structure. This heat treatment produces nanofibers which generally provide the highest electrical conductivity in nanocomposites hence are considered to be better options for smart concrete. The fibres generally become entangled during growth because they are produced in a vapour phase, thus, producing a mesh-like configuration. This raw form is then de-bulked by the manufacturer with a product that is uniform in bulk density allowing accurate compounding into the final products. The de-bulked form is denoted as XT. The loose bundle of the 'XT' carbon nanofiber requires much less energy to achieve dispersion, thus allowing greater retention of fibre length during processing. The surfactant used for dispersion of CNF in water was a high-range polycarboxylate-based water-reducer admixture (superplasticiser) provided by Elkem under the commercial name ViscoFlow 1000.

Mix proportions

A total of five concrete mixtures incorporating different contents of CNF were produced in this study in order to evaluate the effect of carbon nanofibers. The concrete mixture was designed aiming for a target strength of 53MPa; and some mixture trials were tested and a final concrete mix proportions was obtained. Plain Concrete (PC) mixture was dealt as control mixture with no fibres. For other mixtures CNF was added at different dosages by binder volume ranging from 0.25%-1.0%. The content of the mixture was kept constant in all mixtures with W/B (water/binder) ratio of 0.37. Silica fume was kept at 10% by weight of cement and the High Range Water Reducer (HRWR) was used at 0.5% of the binder. The composition of all mixtures is presented in Table 4.

Preparation of CNF and dispersion in mixing water

According to previous research findings, HRWR was used to achieve a better dispersion of CNF in aqueous solution. In this study, the HRWR along with ultrasonication was adopted to achieve a good dispersion of the nano fibres in the liquid medium. As Yazdanbakhsh (2012) states, 'superplasticiser should not be added to the paste during paste mixing and is required to be added to the aqueous solution

to yield the best possible dispersion' of CNFs in water during ultrasonic processing. Therefore, the aqueous solution was made by the following steps:

a) Water + HRWR ; stirred manually
b) CNF was added; stirred manually for about 2 minutes
c) Ultrasonication process

A 20-kHz ultrasonic processor (Vibra-Cell, Model VCX 750, Sonics & Materials) was used to disperse the nano fibres with a 139mm long titanium alloy solid probe with 13mm diameter. The processor was set to operate at an amplitude of 50% at 20s time intervals to prevent overheating of the solution. The CNFs were weighed in a glass container, then water+HRWR liquid was added and stirred manually. The solution of water+HRWR+CNF was sonicated for about 15 min which was the optimum time needed to achieve well-dispersed CNF/water solution at room temperature. Details of the sonication for each batch are presented in Table 5.

Sample preparation

Following the recommendation by the Elkem Materials, the silica fume was added to the mix of fine and coarse aggregate. The mixing procedure for CNFRC concrete was as follows:

a. Coarse aggregate and fine aggregate were added to the mixer and mixed well (2 minutes).
b. Silica fume was added and mixed (2 minutes).
c. Once evenly mixed (a uniform grey colour obtained), cement was added and mixed well (2 minutes).
d. Water+HRWR+CNF was then added under low speed to the mixer and mixed well till the paste uniformity was enhanced (3-5 minutes).

Mechanical properties studied

For each mix, six cylinders and three beams were casted and specimens were tested under uniaxial compression, splitting tensile and flexural loading using ADVANTEST 9 (Controls Group) testing machine.

Compression Test

The compression test was conducted according to BS EN 12390-3:2002 (2002). Since the post-peak behavior of the material was important to this research, the load was applied in a displacement control manner and the strain was monitored in the concrete. The displacement was controlled through displacement transducers attached to the cylindrical specimen in equal angular distances of 120˚. The transducer was hammered into concrete with an initial length of 100mm. they were tightened to concrete and kept in place with an elastic band around all three transducers. The displacement was applied at a rate of 1µm/s.

Flexural test

The flexural test was conducted according to BS EN12390-5:2000 (2000). The beams were 100×100×500mm. The clear span was set to 300mm and the upper bearer distance was set to 100mm. Two displacement transducers at the center of the specimen on both front and back sides of the beam were used to measure the mid span displacement. This test provides a clear means of comparing the post-cracking tensile behavior of various fiber reinforced concretes. The test was conducted under displacement control and the load was applied with a rate of 0.1µm/s. The flexural strength (or maximum tensile stress in the lower fiber of the beam under loading) can be obtained using the BS EN 12390-5:2000 guidelines.

Split tensile test

The uniaxial tension tests have a complex nature, therefore splitting tension tests are usually conducted on cylindrical specimens by compressing the cylinder through a line load applied along its length which can be conducted in a standard concrete compression testing machine. Therefore, for this study the split tensile test was conducted on cylinders with dimension of Ø100×200 mm according to BS EN12390-6:2009 (2009). According to this guidance, a constant loading rate of 1260 N/s was used.

Self-health monitoring

CNF concrete is a material with discontinuous conductive nanofibers (CNF) which creates an electromagnetic field and transforms the non-conductive concrete into a conductive material. For this study, a direct-current four-probe method was adopted to measure the sensitivity of the concrete beam during the flexural beam tests. In this method, four electrodes are embedded within the matrix in which the outer two electrodes are the current pole for passing current, and the inner two electrodes are the voltage poles for measuring the voltage. Therefore, the electrical resistance between the two middle electrodes could be calculated based on ohm's law where: $V=I\times R$ (i.e. V is the voltage (volts, v), R is the resistance (Ohm, Ω) and I is the current (Amp, A)).

Four electrode contacts made with woven copper wire mesh (#16 mesh), with 1.233mm Aperture, and 0.355mm wire diameter were placed symmetrically with respect to the centre along the length of the beam specimens at four planes that were all perpendicular to the stress axis (Figure 1). Before the last 30 seconds of concrete compaction, the electrodes were inserted and clamped to the sides and vibrated for a short while enough to release any possible local entrapped air during insertion of the copper mesh. The outer electrodes were connected to a power supply unit capable of supplying Direct Current (DC) up to 30V. Since the electrical resistance of the concrete varied with elapse of time due to polarization of positive and negative charges (Konsta-Gdoutos and Aza, 2014), direct current was applied for approximately 15 min prior to testing to let the electrical resistance stabilise in concrete. A single concrete strain gauge (PL-60-11, by TML) was attached to both sides of the beam at the centre close to the top surface as shown in Figure 6 to measure the compressive strain of the top fibres of the beam during loading. In order for the metallic elements of the loading rig not to influence the electrical readings, the bottom surface of the samples in contact with the rig rollers was isolated with an electrical resistance tape, as well as the bottom surface of the top roller. The output was then used to correlate with the electrical readings.

The current was kept constant throughout the test at 1mA. The resistivity and the strain along the stress axis of specimens were measured respectively by the data acquisition system and concrete strain gauges during loading. The concrete gauge attached to the surface of the beam and the copper electrodes are

shown in Figure 2. The configuration of wire attachments to the power supply as well as the final beam set up is illustrated in Figure 3. It is important to note that all samples have been tested at the same age and in the same environment. The effect of age of samples and humidity of the environment is an important subject that will be investigated in future research studies.

Results and discussions

This section presents the mechanical properties of CNFRC materials. The results from compression, split tensile, and flexural tests are discussed in the following sub-sections.

Compression test results

The graph in Figure 4 presents the stress-strain relationship for all concrete types, and the compressive strength of cylinders for all types of concrete is shown in Figure 5. For each type, the results of two representative samples are presented. Since the strength of the concrete is dependent on the calcium silicate hydrate (C-S-H) component of the concrete, the nanofibers are expected to reinforce the nanoscale properties of the C-S-H, hence increasing the compressive strength. At the interface, CNF possesses an intimate bonding with the cement matrix due to the Van der Waals forces. The large aspect ratio and stacked-up cone shape and rough edges of the fibers give themselves filament abilities to block and diver micro-cracks, which can slow down crack propagation and formation of the crack network. The increase in compressive strength can be related to two effects:

- *Bridging effect* of the CNF for micro-cracks,
- *Filler effect* for accelerating the hydration reactions of the cementitious materials.

Figure 6 shows the Scanning Electron Microscopic (SEM) images of a cracked CNF concrete sample. Figure 6a shows that the nanofibers are bridging the micro cracks. Figure 6b depicts that some nanofibers have pulled out and fractured at the surface. When the nanofibers are pulled out with the increase in applied loads, energy is dissipated at the nanofibers-matrix interface, resulting in delayed macro crack formation.

From Figure 5, with the addition of only 0.25% of CNF fibers to the concrete, the compressive strength was increased by 30.5%. However, there was an inflection point at 0.5% CNF content, at which the compressive strength of concrete was decreased by 8.5%. This decrease could be attributed to the presence of fiber clumps in concrete matrix and poorer dispersion quality of the CNF solution compared to other CNFRC samples. Although CNFRC0.5 was less effective in enhancing plain concrete post-peak behaviour (Figure 4), it improved the strength by 19.5%, which is comparable to the findings of Sanchez and Sobolev (2010) who found an increase in compressive strength of plain mortar from 30 MPa to 36 MPa (by 20%) using CNF at 0.5% wt. of cement (with W/C=0.365). Compared to the results obtained by Kowald (2004) who used 0.5% CNT in high-strength concrete and found a 12% increase in compressive strength, it can be stated that the CNF incorporated in this study showed slightly better performance than CNT. Li et al. (2005) also obtained a 19% enhancement in compressive strength of mortar by using 0.5% MWCNT.

In this study, the maximum strength was achieved by the addition of 1.0% fibre, with 39% increase in strength. It is worth mentioning that the results for CNFRC0.75 were very close to CNFRC1.0, hence the effect of fibre at a dosage higher than 0.5% became inconspicuous in the case of this experimental program. In the review of the previous work on the compressive strength of CNF composites, it was found that 1.0% CNF by volume of binder increases the cylinder compressive strength by 26.9% (Sivakumar, 2011) which was lower than what was achieved in this research. However, Gao et al. (2009) found that the addition of 0.16% CNF to a self-consolidating concrete (SCC) increases the compressive strength by 40%. The reason for higher enhancement found by them could be the type of the concrete used in their study, suggesting that SCC could possibly better accommodate the dispersion of the fibres when mixed with the cementitious materials and hence achieving a more uniform mixture because of its higher fluidity (due to higher HRWR and water content) resulting in higher strength increase. This is, however, a premise that needs to be further studied in the future.

From the post-peak behaviour of cylinders, it can be seen that CNFRC0.75 and CNFRC1.0 had similar behaviour, and they outperformed other materials in terms of ductility, reaching a strain exceeding 0.004 at failure. CNFRC0.5 reached higher strain despite lower strength compared to CNFRC0.25.

Figure 7 shows specimens of Group B after failure. From the figure, PC and CNFRC0.25 showed the most damage and concrete was broken into pieces, however, CNFRC0.75 and specially CNFRC1.0 showed the least damage, mainly on the concrete surface. It can be concluded that samples with higher fibre dosage (0.75% and 1.0%) were more successful in attaining their integrity and mainly surface damage was observed. The reason for this is because the fibres enhanced the compressive performance of concrete by better filler effect (i.e. creating compacter concrete by filling the voids in the matrix) at higher fiber dosage.

Split tensile test results

The average split tensile strength of all samples for each concrete type is shown in Figure 8. No significant changes were observed in the splitting tensile strength with variation in the CNF percentage. However, compared to PC this mechanical property was increased by 24.2% when 1.0% CNF was added to the concrete. Amongst the CNF concrete samples, both 0.75% and 1.0% CNF fibre had the greatest effect on the concrete and their effect was almost similar. Addition of 0.25% CNF in the concrete resulted in 22.2% increase in split tensile strength, which is close to the findings of Gay and Sanchez (2010) who found 26% increase in tensile strength of the reinforced cement paste with 0.2% CNF. It can be concluded that the effect of CNF within concrete could compete with its effect in cement paste or cement mortar. On the other hand, the direct tensile strength of 0.3% (wt. of binder) CNF reinforced UHPC tested by Meng and Khayat (2016) showed 56% increase in the strength, and Sivakumar (2011) achieved 66.6% increase in split tensile strength of SCC with 1.0% CNF by volume of binder. The different results obtained by these researchers could be due to the different concrete type used in their study, namely UHPC (which is more compact than PC) and SCC (which has higher fluidity than PC) respectively. As mentioned beforehand, this comparison suggests that the effect of CNF could vary within different concrete types and further studies regarding this issue are recommended. All samples failed by a crack through the centre of the cylinders and splitting the cylinder into two pieces as shown in Figure 9.

Flexural test results

The flexural strength of each sample was calculated according to BS EN 12390-5:2000 and the average strength is presented in Figure 10. From this figure, the change in the flexural strength shows the same general trend as compressive strength and split tensile strength for CNFRC with an inflection point at 0.5% fibre dosage. From the three samples that were tested, the load-displacement relationship of one beam from each mix, representing the behaviour of the concrete is shown in Figure 11.

According to both Figures 10 and 11, it is evident that the addition of CNF has increased the flexural strength of the plain concrete by 63%, 35.3%, 52.5%, and 85% respectively with fibre dosage of 0.25%, 0.50%, 0.75% and 1.0%. From reviewing previous researches, a 55.5% increase in the flexural strength of the cement paste was found with the addition of CNF at 0.1 wt.% of cement (Tyson et al., 2011). This fibre dosage was close to the CNFRC0.25 of this research with an equivalent CNF dosage at 0.17 wt.% of cement. It is seen that both results are somewhat close considering that the higher fiber volume fraction used in CNFRC0.25 might be the reason for higher effect (63%) on the flexural strength. When Tyson et al. (2011) doubled the amount of fibre dosage (0.2 wt.%), the flexural strength decreased by 30%. This phenomenon also occurred in this study between CNFRC0.25 and CNFRC0.5; in which the compressive strength decreased by 17.3% as the amount of fibre was doubled.

Li et al. (2005) achieved a 25% increase in the flexural strength of cement mortar by the addition of 0.5% MWCNT. The results obtained in this study for an equivalent amount of CNF in concrete was 35.3%, which suggests that CNF could compete with CNT and perform better within the concrete matrix.

From the strength point of view, it is evident that the concrete with 1.0% fibre was the strongest with a flexural strength of 6.30 MPa. The performance of CNFRC1.0 in this study outperformed the results found by Sivakumar (2011), who found an increase of 38% in flexural strength of SCC when 1% CNF by volume of binder was used. Also, Meng and Khayat (2016) reported a 46% increase in flexural strength of UHPC reinforced with 0.5% micro steel fibre and 0.3% CNF. This enhancement in flexural strength could be of great advantage for the behaviour of concrete members at the structural level. Overall, the trend of change in compressive strength, flexural strength, and split tensile strength from

0.5% to 1.0% in this study agrees with the findings of Sivakumar (2011) for CNF reinforced SCC who found an increasing trend in all mechanical properties.

Interestingly, contrary to what one might presuppose that the 0.25% fibre addition could have the least effect on the behaviour of the material as opposed to higher fibre concentrations; it was more effective than 0.5% and 0.75% fibre concentrations in the concrete matrix in increasing the flexural strength. A possible reason is that due to the lower fibre concentration, agglomeration of fibres was greatly prevented and better dispersion was achieved for this material. However, according to the load-displacement graph, CNFRC0.25 did not show great ductility compared to other CNFRCs. The material showed more brittle behaviour after reaching the maximum strength followed by sample breakage regardless of its higher strength capacity.

CNFRC0.5, CNFRC0.75, and CNFRC1.0 showed relatively high displacement capacity compared to PC which means that these materials had much higher ductility. The displacement at failure of the plain concrete specimen is about 0.08mm; while the displacements at failure of the specimens reinforced with 0.5%, 0.75%, and 1% CNF are respectively 0.22mm, 0.24mm, and 0.19mm. This corresponds to an amplification factor between 2.38 and 3, indicating a significant improvement in ductility. This can be attributed to better nano-crack and micro-crack control due to a higher concentration of fibres as opposed to CNFRC0.25. During the post-peak stage, CNFRC1.0 showed higher load level than other samples and at the mid-span deflection of 0.12 mm, the capacity of the sample reached the same capacity as CNFRC0.75. At this stage, both CNFRC0.75 and CNFRC1.0 had higher loading capacity compared to CNFRC0.5, hence higher energy dissipation was obtained for 0.75% and 1.0% CNF samples. On the other hand, it is interesting to note that the maximum displacement achieved by 0.5% CNF reinforced concrete was higher than 1.0% CNF sample.

Although it was assumed that better dispersion of 0.25% fibres caused higher flexural strength than 0.5% and 0.75% fibre, it should be emphasised that the dispersion of other samples was also satisfactory since there was an apparent improvement in the behaviour of the concrete in terms of strength, ductility, and energy dissipation capacity, which was manifested by the post-peak behaviour. This is due to the

presence of higher fibre dosage. Overall, it is believed that the CNF embedded in the paste along with the network created by CNF inside of the pockets (referring to clumps that might not have been fully dispersed, and be formed inside the paste followed by being introduced into the concrete matrix) may have limited the propagation of the cracks when 1.0% fibre is used, allowing specimens to retain some significant flexural capacity over the plain concrete.

Figure 12 shows the failure of CNFRC beam samples after the test. While the figure shows a single crack for the CNFRC specimens, the initiation of the crack was much delayed for the specimens reinforced with CNF, and the crack propagation was also much slower than in the case of plain concrete. This resulted in a smaller crack width at failure, as can be seen for sample CNFRC0.5, where the developed crack was very thin and the beam remained mostly intact. This failure explains the load-displacement behaviour of the beam and its higher ductility. Also, CNFRC1.0 showed thin crack width towards the top of the beam. CNFRC0.25 had a full breakage shortly after reaching the maximum strength and the beam was split into two pieces (Figure 12a).

Self-health monitoring results

To investigate the self-health monitoring capability of CNF concrete and quantify this property for each sample, the following time histories are plotted and compared for each concrete type.

- Load vs. time
- Compressive strain vs. time
- Measured electrical resistance vs. time

These plots are shown in Figures 13 and 14 for PC, CNFRC0.25, CNFRC0.5, CNFRC0.75, and CNFRC1.0 respectively. Additionally, the average value of initial electrical resistance for CNFRC samples after stabilisation of electrical circuit for 15 min prior to loading is tabulated in Table 6. From the results, increasing the fibre dosage decreased the electrical resistance of the concrete evidently. For the plain concrete, no relation could be detected between the resistance and strain. However, a good correlation was qualitatively observed for CNFRC between strain and electrical resistance during loading.

Considering the CNFRC0.25 results, as the load increased, the compressive strain measured by the strain gauge in the centre of the beam at the top also increased, while the calculated resistance was decreasing inversely proportional to the strain. Both CNFRC0.5 and CNFRC0.75 results (Figure 14) showed similar behaviour regarding the relationship between resistance of the material with the load and strain. The variation in resistance (R) value was varying with strain following the same trend. The change in resistance was however in reverse to the strain. For all samples, a trend was found in which with increasing compressive strain, the resistance decreased and with decreasing compressive strain, the resistance increased. This is because under compressive stress, the fibres in the concrete get closer to each other as the material is compressed, hence the conductive network becomes stronger resulting in decreased electrical resistance. On the other hand, the conductive network becomes weak either due to the fibers getting apart from each other by reducing compressive stress (for e.g. unloading specimen) or due to micro-cracks interrupting the circuit, thus the resistance increases gradually. The decrease in electrical resistance for samples can be spotted during the post-peak stage. This could be due to the development of micro-cracks during this stage.

During the test of sample CNFRC1.0, the beam reached its highest load carrying capacity very quickly and it fractured within 30 seconds. Despite the short duration of the test, the change in electrical resistance was promptly responsive to the change in strain. This result can confirm that the CNFRC is apt to measure rapidly varying strain responses. This also manifests the potential of CNFRC as a damage sensor, by a dramatic change in the resistance at loading instances as early as the maximum load, hence providing timely failure warnings. This phenomenon was also claimed for cement paste by Materazzi et al. (2013).

The results presented here can thus contribute to extending the known strain-sensing capability of the CNF cementitious composites to the CNF reinforced concrete (CNFRC). To better understand the relation between the strain and the electrical resistance, electrical resistance variation (ERV) is analysed for each concrete and presented in the next subsection.

Electrical Resistance Variation (ERV)

Piezoresistivity of the CNFRC is expressed using fractional change (ERV) in resistance. The current was constant (A) and the initial voltage reading (V_0) was recorded and hence the initial electrical resistance R_0 was calculated for each sample. Subsequent voltage values were recorded every second at the same time as the strain was recorded during the test. Therefore, each strain value at every time point i had corresponding values of voltage recorded as V_i. The electrical resistance R_i and electrical resistance variation, *ERV,* were calculated as follows:

$$R_0 = V_0 / A, \tag{1}$$

$$R_i = V_i / A \tag{2}$$

$$ERV = (R_i - R_0)/R_0 \tag{3}$$

ERV vs. strain is plotted and presented in Figure 15 for all concrete types. The linear function for the best-fit linear trend line, correlating the ERV and the strain is also presented in this figure along with the correlation coefficient (R^2). The correlation coefficient of the best-fit line to the data is a measure of the linear distribution of the data. If the data has a strong linear distribution, (R^2) is closer to 1.

From the plot above, it is apparent that when loading samples started, the strain started to increase and the absolute value of ERV increased from zero simultaneously with the strain. The ERV had negative sign since the resistance decreased under compressive strains; and since the absolute value of the ERV is of importance to this discussion, henceforward the ERV sign is neglected in the magnitude comparisons. The maximum ERV for CNFRC cases occurred near a strain of 150με. It is evident that ERV was constant for PC, showing no variation in resistance, while it was increasing for all volume fractions of CNF as the compressive strain increased. The maximum electrical resistance variation was directly related to CNF concentration and according to the figure, it can be concluded that the tunnel conductivity effect of the CNFRC increases with increasing the fibre concentration as the maximum ERV value increased from 0.06 to 0.17 when fibre dosage increased from 0.25% to 1.0%.

The ERV versus strain relationship for CNFRC0.25 exhibited deviation from the perfect linear behaviour at a strain of about 70 με, while other CNFRC maintained their original slope, and an almost

linear relationship between ERV and compressive strain could be detected for 0.5%, 0.75% and 1.0% CNFRC. This can be determined from the R^2 coefficient values for CNFRCs, which was the smallest (R^2 = 0.902) for CNFRC0.25. On the other hand, other CNF concentrations showed a very good linear correlation coefficient (i.e. R^2 closer to 1).

The ERV was comparatively steady when the fibre concentration was 0.75% and 1.0% and the maximum ERV for these were 0.17 and 0.19 respectively. This was close to the values found in the literature (Gao et al., 2009) for SCC where using CNF fibres at 0.70%, 1.0% and 2.0% lead to a maximum ERV value of 0.20, 0.21 and 0.25 respectively. In another study (Camacho-Ballesta et al., 2016), the maximum ERV for 0.25% and 0.5% CNT cement paste was 0.05 and 0.14 respectively which are close to the values found in this study for 0.25% CNF (ERV_{max}= 0.06) and 0.5% CNF (ERV_{max}= 0.13) in concrete. The close values of the ERV for specific fibre volume fractions of these studies, considering the different matrix used, could lay down the foundation of a finding which suggests that from a certain volume fraction of CNF (i.e. nanofibers) in concrete, there exists a specific range of conductivity that can be expected from the material, subjected to satisfactory dispersion of the nanofibers. However, this hypothesis needs to be further investigated with more experiments.

Conclusions

This paper aimed to fill an important gap in the literature by comparing the mechanical performance of CNFRC with plain concrete and evaluate the effect of CNF at different volume fractions (0-1.0% by the volume of binder) on the compressive, tensile and flexural performance of concrete. In addition, a qualitative assessment of the electrical data obtained for a CNFRC beam was conducted to investigate its self-sensing property. The following conclusions were made from the results:

- Addition of 1.0% CNF (amongst 0.25%, 0.5% and 0.75% volume fractions) into concrete resulted in the highest compressive strength improvement by 39% as well as better post-peak behaviour for stress-strain relationship under uniaxial compression. Also, this amount of fibre showed the best flexural strength with the magnitude of 6.30 MPa. This increase in the flexural

capacity of the beam with the addition of 1.0% fibres showed that the nanofibers were effective in increasing the flexural capacity of the beam to a great extent.

- The flexural strength was more influenced by CNF dosage amongst the CNFRC samples as opposed to other mechanical properties; whereas, the split tensile strength was the least affected by varying the CNF dosage. Having said that, the split tensile strength was improved by 22.2% with the addition of only 0.25% volume fraction of CNF.
- The peak displacement of concrete under four-point bending test was improved for CNFRC mixes. The greatest achievement was observed for 0.5% and 1.0% CNF reinforced concrete up to 170% higher than PC, which is crucial to structural applications in which higher ductility and strain capacity to failure is needed.
- Regarding the damaged samples, specimens with 0.75% and 1.0% fibre in concrete showed better integrity in compression test, and surface damage was observed rather than severe crushing and explosion of the cylinder samples.
- From the self-sensing point of view, increasing the fibre dosage from 0.25% to 1.0% decreased the electrical resistance of the concrete by almost 50% from 8.78 kΩ to 4.19 kΩ.
- The electrical resistance of the CNFRC showed a reverse relationship with compressive strain. As the compressive strain decreased, the resistance increased, while with increasing compressive strain, the resistance decreased.
- The electrical resistance variation (ERV) for PC showed no relation with applied strain, while the ERV for all CNFRC had a linear relation with compressive strain prior to reaching the ultimate load with the correlation coefficients (R^2) above 0.9.

Acknowledgments

The first author is grateful to the financial support obtained by City, University of London. The authors also wish to thank the technical staff of the Structural Laboratory at City, University of London, in particular the director Dr. B. McKinley.

References

Azhari F and Banthia N (2017) Carbon Fiber-Reinforced Cementitious Composites for Tensile Strain Sensing. ACI Materials Journal 114(1): 129-136.

BS EN 12390-5:2000 (2000) Testing hardened concrete; Flexural strength of test specimens. BSI, London.

BS EN 12390-3:2002 (2002) Testing hardened concrete; Compressive strength of test specimens. BSI, London.

BS EN 12390- 6:2009 (2009) Testing hardened concrete; Tensile splitting strength of test specimens. BSI, London.

Camacho-Ballesta C, Garces O and Zornoza E (2016) Performance of cement based sensors with CNT for strain. Advanced Cement Research 28(4): 274-284.

Cao J and Chung D (2001) Carbon fiber reinforced cement mortar improved by using acrylic dispersion as an admixture. Cement & Concrete Research 31(11): 16331637.

Dalla P, Dassios K, Tragazikis I, Exarchos D and Matikas T (2016) Carbon nanotubes and nanofibers as strain and damage sensors for smart cement. Materials Today Communications 8: 196-204.

Galao O, Baeza F, Zornoza E and Garces P (2014) Strain and damage sensing properties on multifunctional cement composites with CNF admixture. Cement & Concrete Composites 46: 90-98.

Gao D, Sturm M and Mo Y (2009) Electrical resistance of carbon-nanofiber concrete. Smart Materials and Structures, 18(9): 095039.

Gay C and Sanchez F (2010) Performance of Carbon Nanofiber-Cement Composites with a High-Range Water Reducer. Transportation Research Record: Journal of the Transportation Research Board 2142: 109-113.

Howser R, Dhonde H and Mo Y (2011) Self-sensing of carbon nanofiber concrete columns subjected to reversed cyclic loading. Smart Materials and Structures 20(8): 085031.

Kim H, Nam I and Lee H (2014) Enhanced effect of carbon nanotube on mechanical and electrical properties of cement composites by incorporation of silica fume. Composite Structures 107: 60-69.

Konsta-Gdoutos K and Aza C (2014) Self sensing carbon nanotube (CNT) and nanofiber (CNF) cementitious composites for real time damage assessment in smart structures. Cement & Concrete Composites 53: 162-169.

Kowald T (2004) Influence of surface-modified carbon nanotubes on ultra-high performance concrete. in Proceedings of International Symposium on Ultra High Performance Concrete, Kassel, Germany.

Li G, Wang P and Zhao X (2005) Mechanical Behaviour and Microstructure of Cement Composites Incorporating Surface-Treated Multi-Walled Carbon Nanotubes. Carbon 43(6): 1239-1245.

Matterazzi A, Ubertini F and D'Alessandro A (2013). Carbon nanotube cementbased transducers for dynamic sensing of strain. Cement & Concrete Composites 37: 2-11.

Meng W and Khayat K (2016) Mechanical properties of ultra-high-performance concrete enhanced with graphite nanoplatelets and carbon nanofibers. Composites Part B 107: 113-122.

Metaxa Z, Konsta-Gdutous M and Shah S (2013) Carbon nanofiber cementitious composites-effects of debulking procedure on dispersion and reinforcing efficiency. Cement and Concrete Composites, 36: 25-32.

Noiseux-Lauze G and Akhras G (2013) Structural health monitoring using smart nano cement sensors. in International workshop on smart materials, structures NDT for the energy industry, Calgary, Alberta, Canada.

“Pyrograf” Applied Science Inc, [Online]. Available: http://apsci.com/?page_id=19. [Accessed 16 April 2013].

Rhee I and Roh Y (2013) Properties of normal-strength concrete and mortar with multi-walled carbon nanotubes. Magazine of Concrete Research 65(16): 951-961.

Salvetat J and Kuik A (1997) Electronic and Mechanical Properties of Carbon Nanotubes. Advanced Materials 22(7): 161-167.

Sanchez F and Ince C (2009) Microstructure and macroscopic properties of hybrid carbon nanofiber/silica fume cement composites. Composites Science and Technology 69(7-8): 1310-1318.

Sanchez F and Sobolev K (2010) Nanotechnology in concrete – A review. Construction and Building Materials 24(11): 2060-2071.

Sasmal S, Ravivarman N, Sindu B and Vignesh K (2017) Electrical conductivity and piezo-resistive characteristics of CNT and CNF incorporated cementitious nanocomposites under static and dynamic loading. Composites: Part A 100: 227-243.

Sivakumar M (2011) Performance characteristics of Carbon Nanofiber Blended Self Compacting Concrete. International Journal of Avanced Structural Engineering 3(2): 179-186.

Tyson B, Abu Al-Rub R, Yazdanbakhsh A and Grasley Z (2011) Carbon Nanotubes and Carbon Nanofibers for Enhancing the Mechanical Properties of Nanocomposite Cementitious Materials. Journal of Materials in Civil Engineering 23(7): 1028–1035.

Wen S and Chung D (2001) Uniaxial compression in carbon fiber-reinforced cement, sensed by electrical resistivity measurement in longitudinal and transverse directions. Cement and Concrete Research 31(2): 297-301.

Yazdanbaksh A (2012) Production, Characterization, And Mechanical Behavior of Cementitious Materials Incorporating Carbon Nanofibers. Texas A&M University, Texas.

Yazdanbakhsh A, Grasley Z, Tyson B and Abu Al-Rub R (2010) Distribution of Carbon Nanofibers and Nanotubes in Cementitious Composites. Journal of the Transportation Research Board, Transportation Research Board of the National Academies 2142: 89-95.

Yazdanbakhsh A, Grasley Z, Tyson B and Abu Al-Rub R (2009) Carbon Nano Filaments in Cementitious Materials: Some Issues on Dispersion and Interfacial Bond. Nanotechnology of Concrete: The Next Big Thing Is Small.

Yazdani N and Mohanam V (2014) Carbon Nano-Tube and Nano-Fiber in Cement Mortar: Effect of Dosage Rate and Water-Cement Ratio. International Journal of Material Science (IJMSCI) 4(2): 45-52.

Notation

A: Electrical Current

ERV: Electrical Resistance variation

R_0: Initial Electrical Resistance

R_i: Electrical Resistance at time i

V_0: Initial Voltage Reading

V_i: Voltage Reading at time *i*

Table 1: Properties of CNT and CNF

Fiber Type		Typical Characteristics					
		Physical Properties			Mechanical Properties		Cost
		Diameter (nm)	Length	SSA	Young's Modulus	Tensile strength	
CNT	**SWCNT**	0.3-2	>200 nm	>300 m^2/g	1 TPa	60 GPa	~£110/g* (EliCarb)
	MWNT	20-80	1-20 µm	250-300 m^2/g			~£50/g* (EliCarb)
CNF		60-200	20-100 µm	50-60 m^2/g	400 GPa	7 GPa	~ £0.43/g**

Table 2: Properties of silica fume

	SiO_2	Retention on 45μm sieve	Bulk Density (Undensified) (Kg/m^3)	Specific surface (m^2/g)	Mean particle size (μm)
Silica Fume (Elkem 940U)	> 90%	< 1.5%	200-350	15-30	0.15

Table 3: Properties of CNF - PR-19-XT-LHT

Fiber type	Fiber name	Average Diameter (nm)	Average length (μm)	Surface area (m2/gm)	Dispersive Surface Energy (mJ/m 2)	Bulk Density (Kg/m^3)
CNF	Pyrograf-III PR-19-XT-LHT	150	50-200	20-30	120-140	16-48

Table 4: Details of concrete mixture proportions per m^3 of concrete

Concrete Mix	W/B	CA (kg)	FA (kg)	Binder (B)		CNF		HRWR (kg)	W (kg)	Slump (mm)
				C (kg)	Silica Fume (kg)	%	(kg)			
PC	0.37	918	955.5	360	36	0.0	0.0	2	146	85
CNFRC0.25	0.37	918	955.5	360	36	0.25	0.63	2	146	125
CNFRC0.5	0.37	918	955.5	360	36	0.5	1.26	2	146	90
CNFRC0.75	0.37	918	955.5	360	36	0.75	1.90	2	146	70
CNFRC1.0	0.37	918	955.5	360	36	1.0	2.50	2	146	50

Notation: CA=coarse aggregate, FA= fine aggregate, C=Cement, SF= silica fume, CNF= carbon nanofiber, HRWR= high range water reducer, W= water.

Table 5: Sonication properties of CNFRC mixtures

CNF %	CNF/W (%)	W+HRWR (ml)	Sonication Energy (J)	t (s)	Watt (J/s)	(Watt/ml)
0.25	0.43	2426.5	36375	270	134.72	0.056
0.50	0.86	2640	91777	600	152.96	0.058
0.75	1.30	3058.7	86330	600	143.88	0.047
1.0	1.71	4068.4	134814	540	244.1	0.060

Table 6: Initial electrical resistance of CNFRC prior to loading

	CNFRC0.25		**CNFRC0.5**		**CNFRC0.75**		**CNFRC1.0**	
Initial R (kΩ)	8.76	8.80	7.9	8.33	5.86	5.86	4.07	4.30
Average (kΩ)	8.78		8.12		5.86		4.19	

FIGURE CAPTIONS

Figure 1: SHM beam specimen layout, b. Equivalent circuit diagram for direct-current four-pole method

Figure 2: (a) Concrete gauge; (b) copper electrodes

Figure 3: (a) Four-pole method configuration; (b) Final beam test set up

Figure 4: Compressive stress-strain relationship

Figure 5: Compressive strength results

Figure 6: SEM images of CNF concrete specimens

Figure 7: Sample failure after compression test: (a) PC; (b) CNFRC0.25; (c) CNFRC0.5; (d) CNFRC0.75; (e) CNFRC1.0; (f) CNFRC1.0

Figure 8: Split tensile strength results

Figure 9: Split tensile failure of cylinders: (a) CNFRC0.25; (b) CNFRC0.75

Figure 10: Flexural strength results

Figure 11: Four-point bending load-displacement graphs

Figure 12: Flexural beam test samples after failure: (a) CNFRC0.25; (b) CNFRC0.5; (c) CNFRC0.75; (d) CNFRC1.0

Figure 13: Time history results for CNFRC

Figure 14: Time history results for CNFRC

Figure 15: ERV vs. strain for all concrete types

TABLE CAPTIONS

Table 1: Properties of CNT and CNF

Table 2: Properties of silica fume

Table 3: Properties of CNF - PR-19-XT-LHT

Table 4: Details of concrete mixture proportions per m^3 of concrete

Table 5: Sonication properties of CNFRC mixtures

Table 6: Initial electrical resistance of CNFRC prior to loading

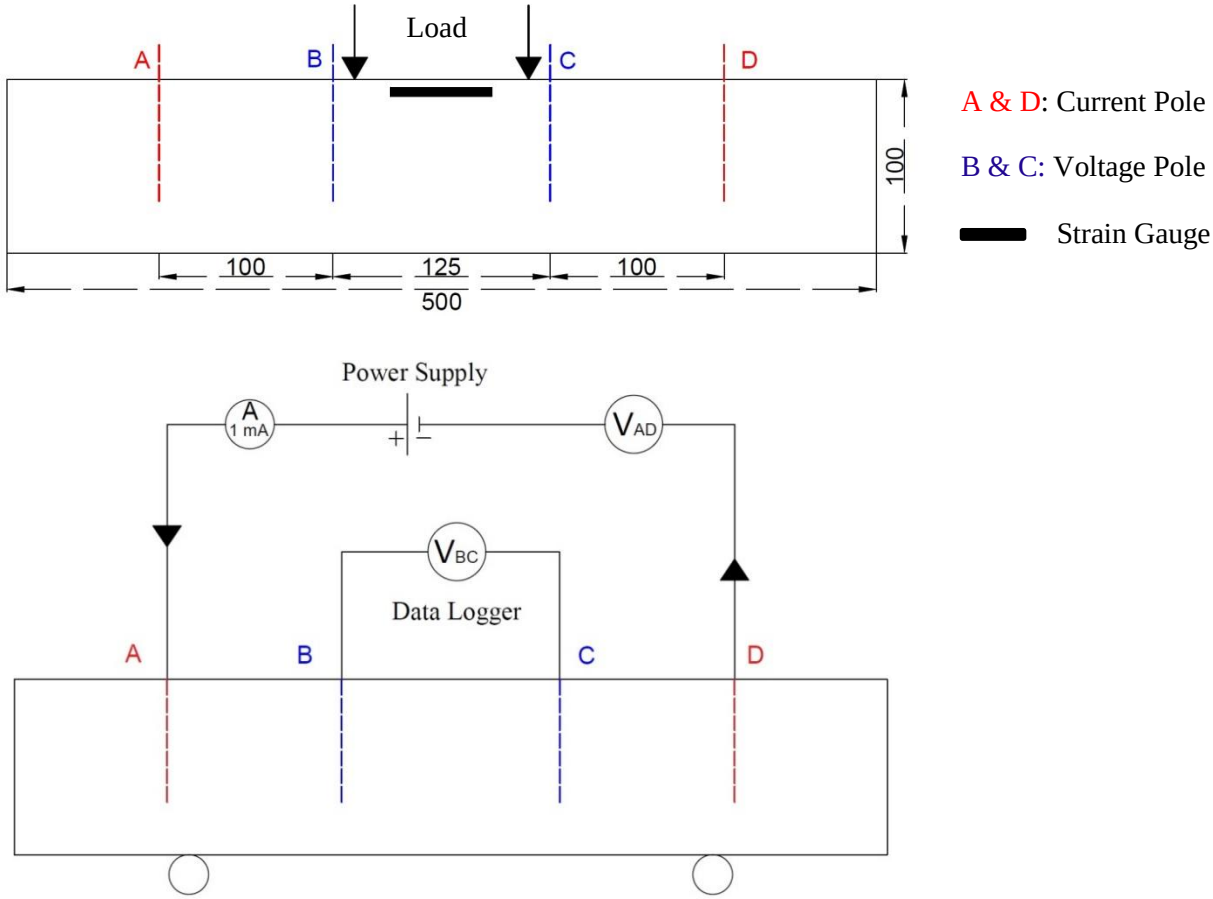

Figure 1: SHM beam specimen layout, b. Equivalent circuit diagram for direct-current four-pole method

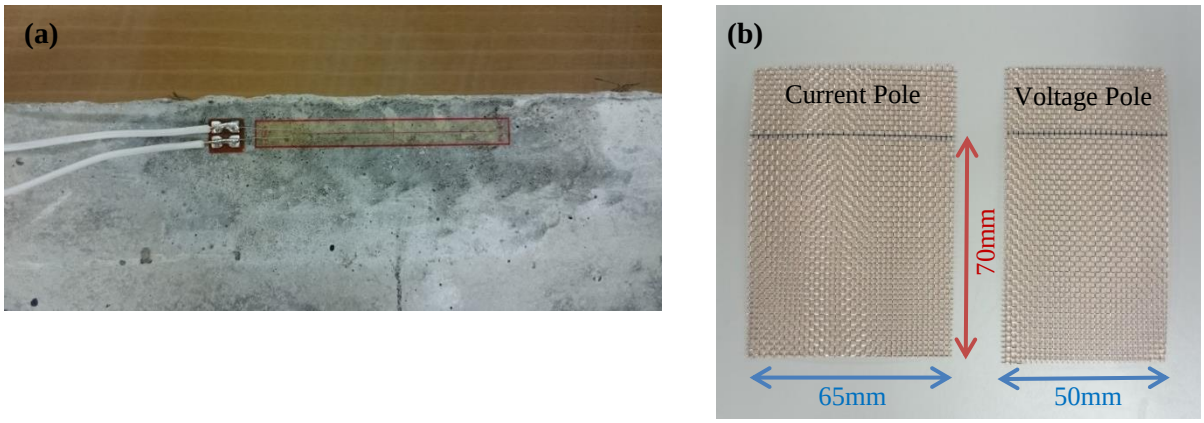

Figure 2: (a) Concrete gauge; (b) copper electrodes

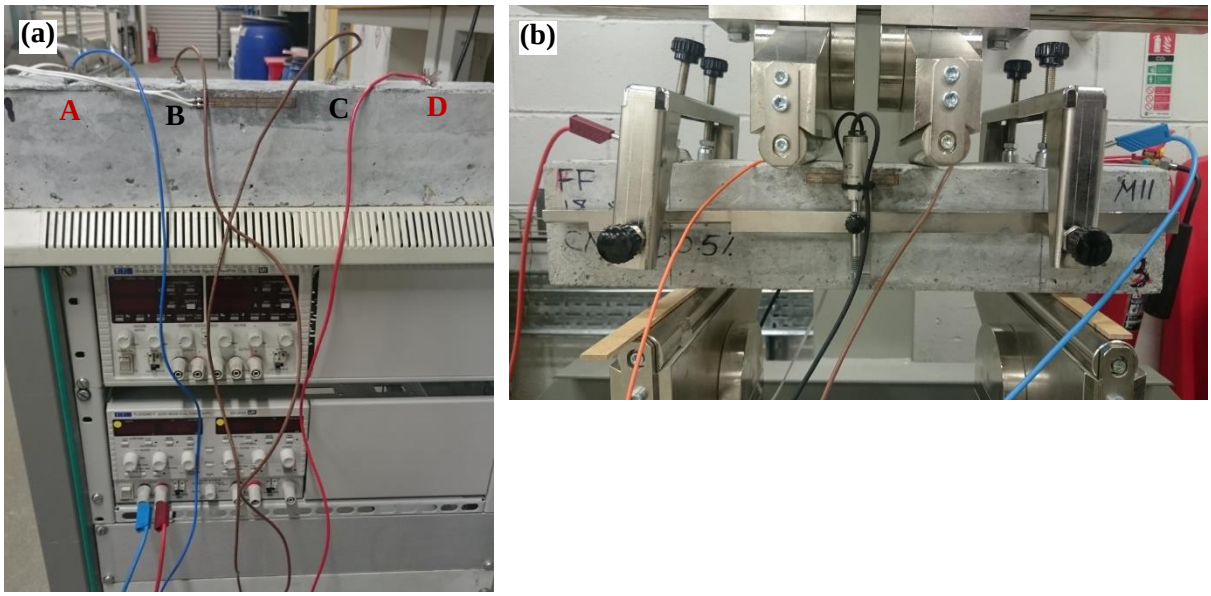

Figure 3: (a) Four-pole method configuration; (b) Final beam test set up

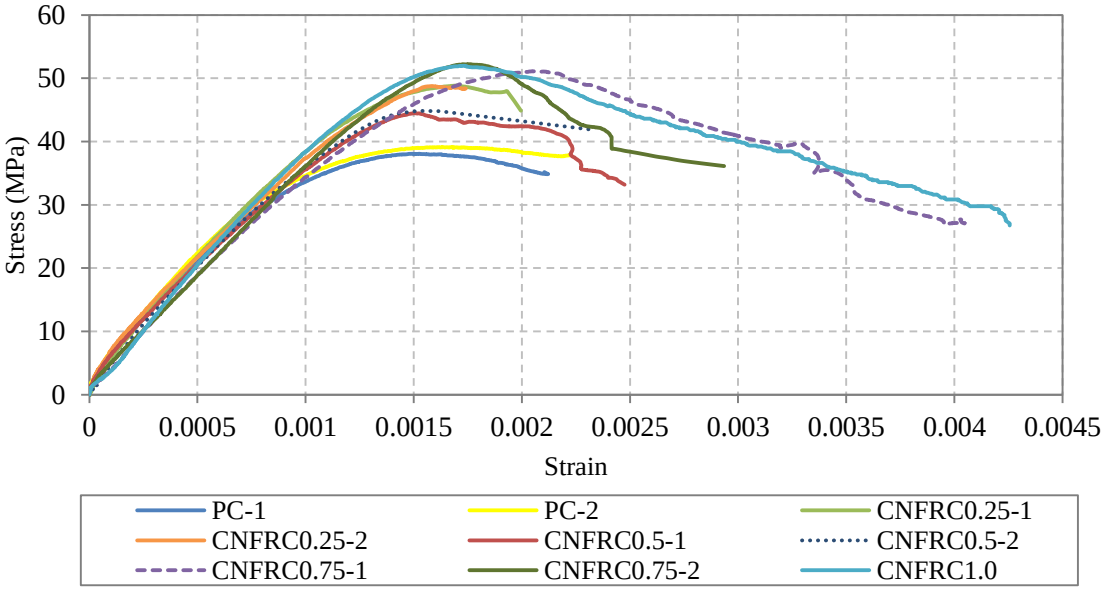

Figure 4: Compressive stress-strain relationship

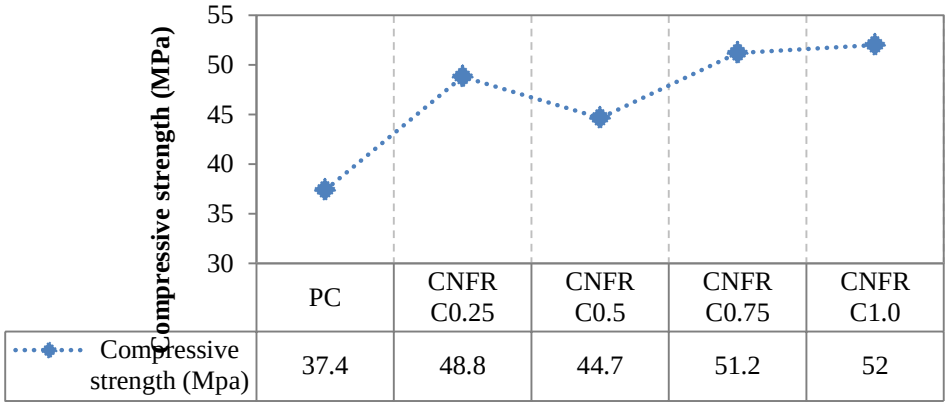

Figure 5: Compressive strength results

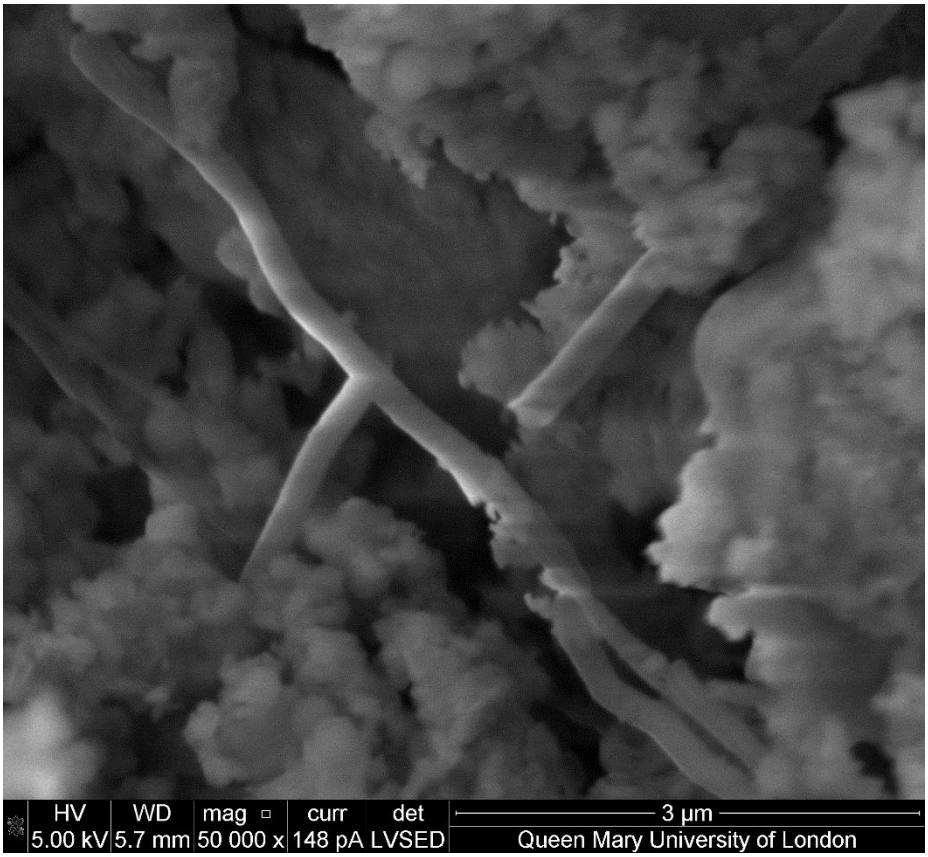

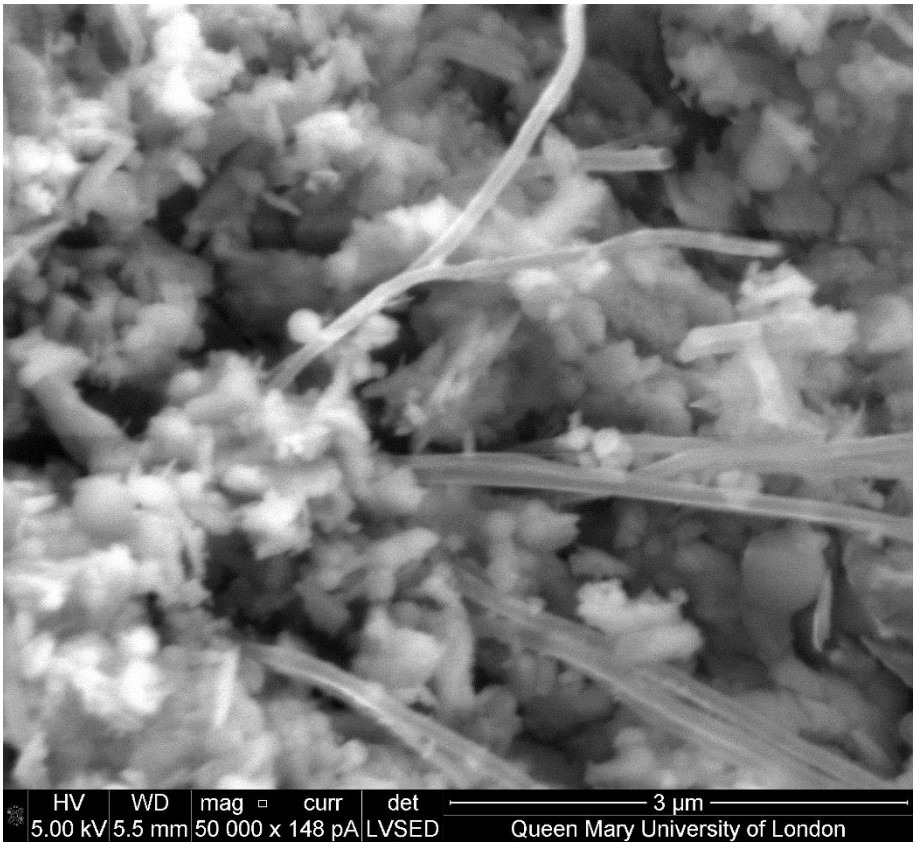

Figure 6: SEM images of CNF concrete specimens

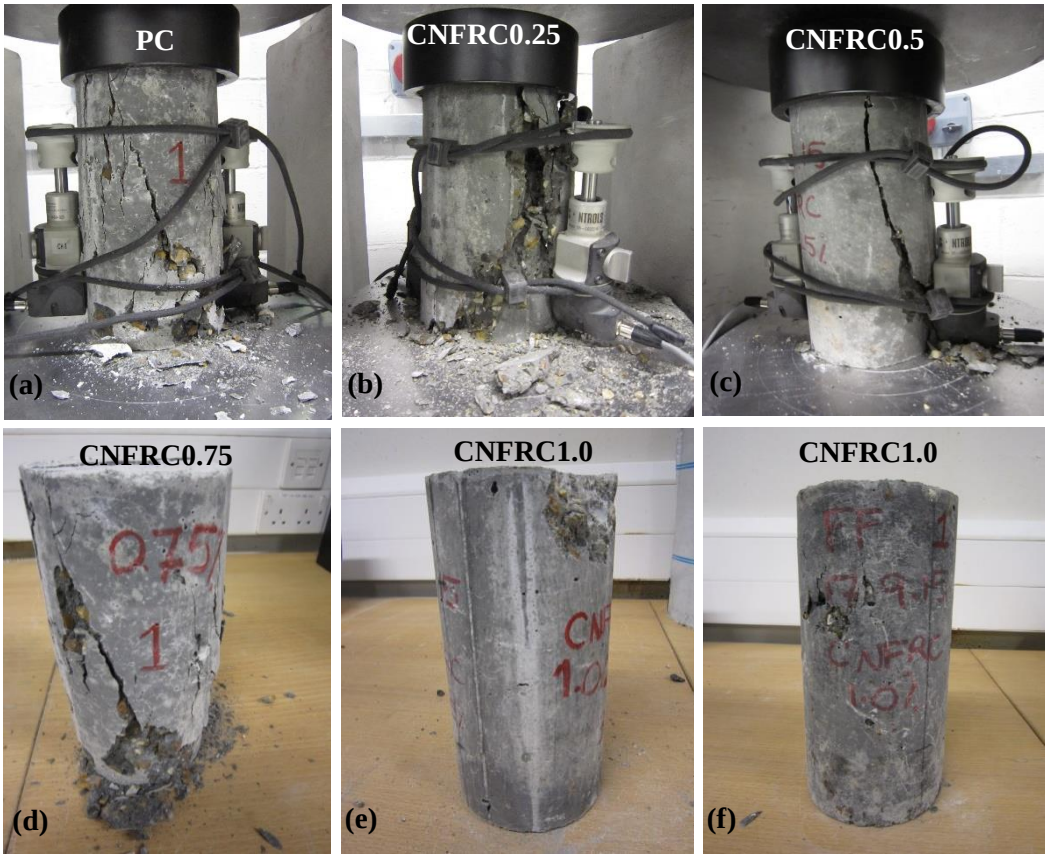

Figure 7: Sample failure after compression test: (a) PC; (b) CNFRC0.25; (c) CNFRC0.5; (d) CNFRC0.75; (e) CNFRC1.0; (f) CNFRC1.0

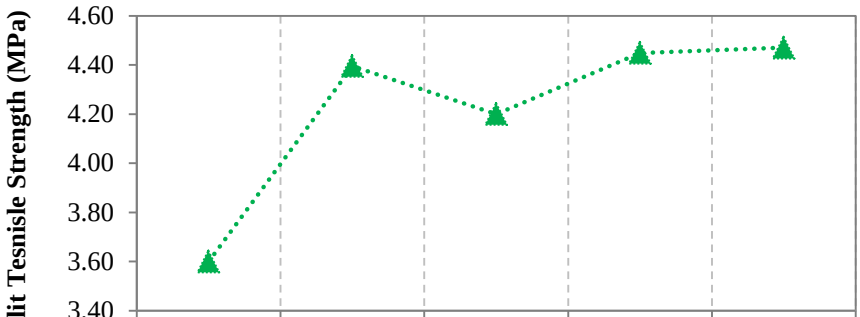

Split Tensile Strength (Mpa)	3.60	4.40	4.20	4.45	4.47

Figure 8: Split tensile strength results

Figure 9: Split tensile failure of cylinders: (a) CNFRC0.25; (b) CNFRC0.75

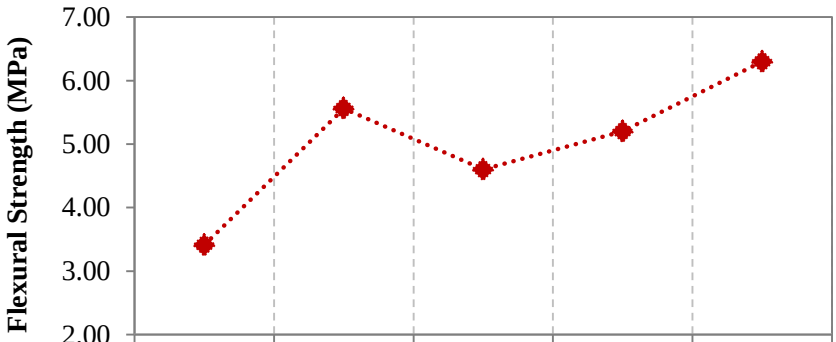

	PC	CNFRC 0.25%	CNFRC 0.5%	CNFRC 0.75%	CNFRC 1.0%
Flexural Strength (Mpa)	3.41	5.56	4.60	5.20	6.30

Figure 10: Flexural strength results

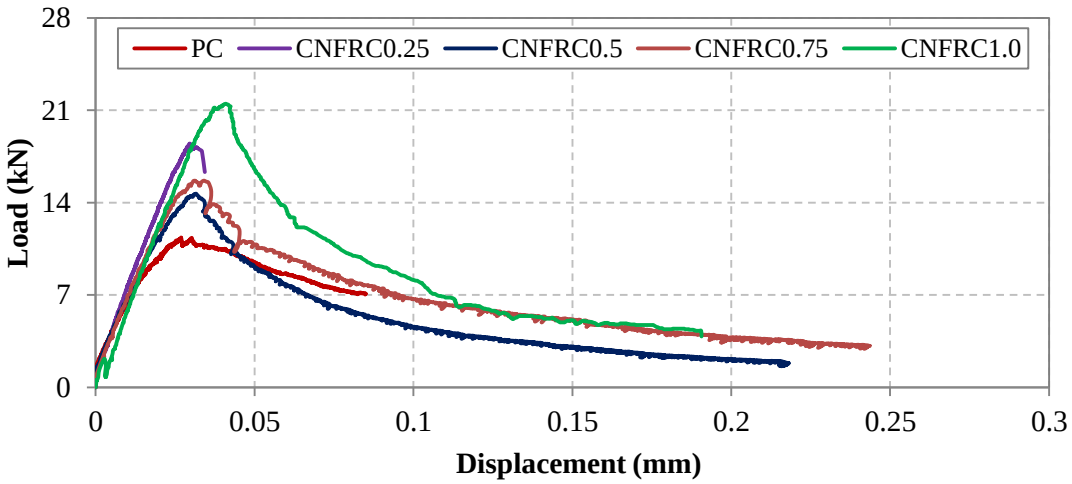

Figure 11: four-point bending load-displacement graphs

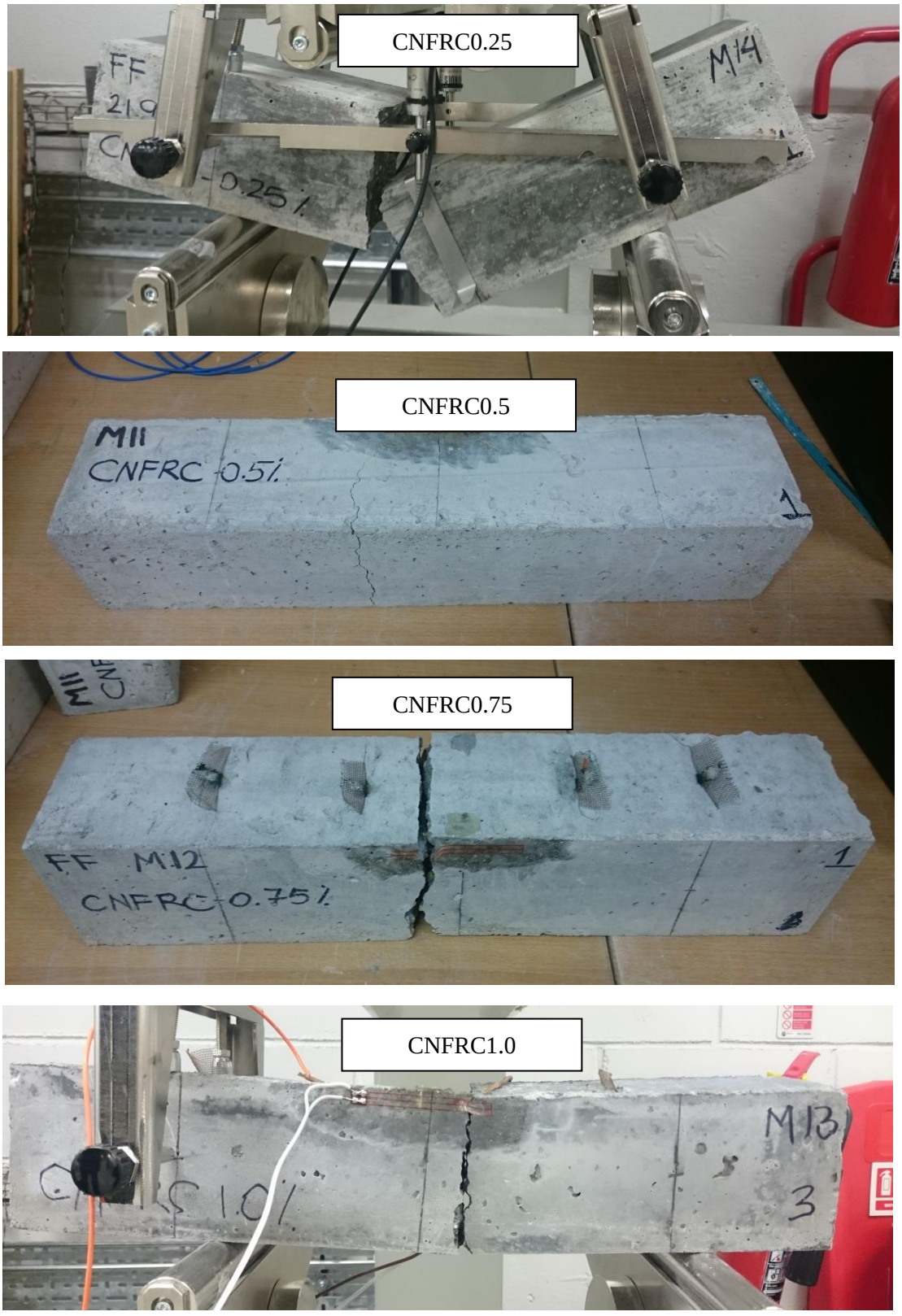

Figure 12: Flexural beam test samples after failure: (a) CNFRC0.25; (b) CNFRC0.5; (c) CNFRC0.75; (d) CNFRC1.0

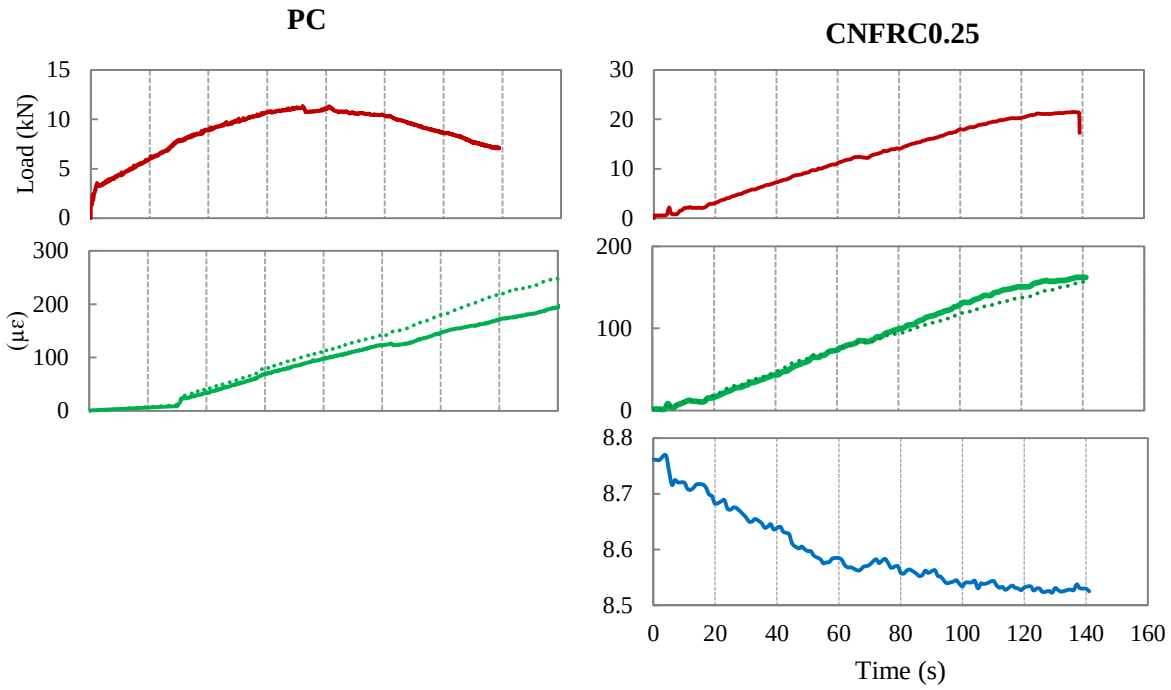

Figure 13: Time history results for CNFRC

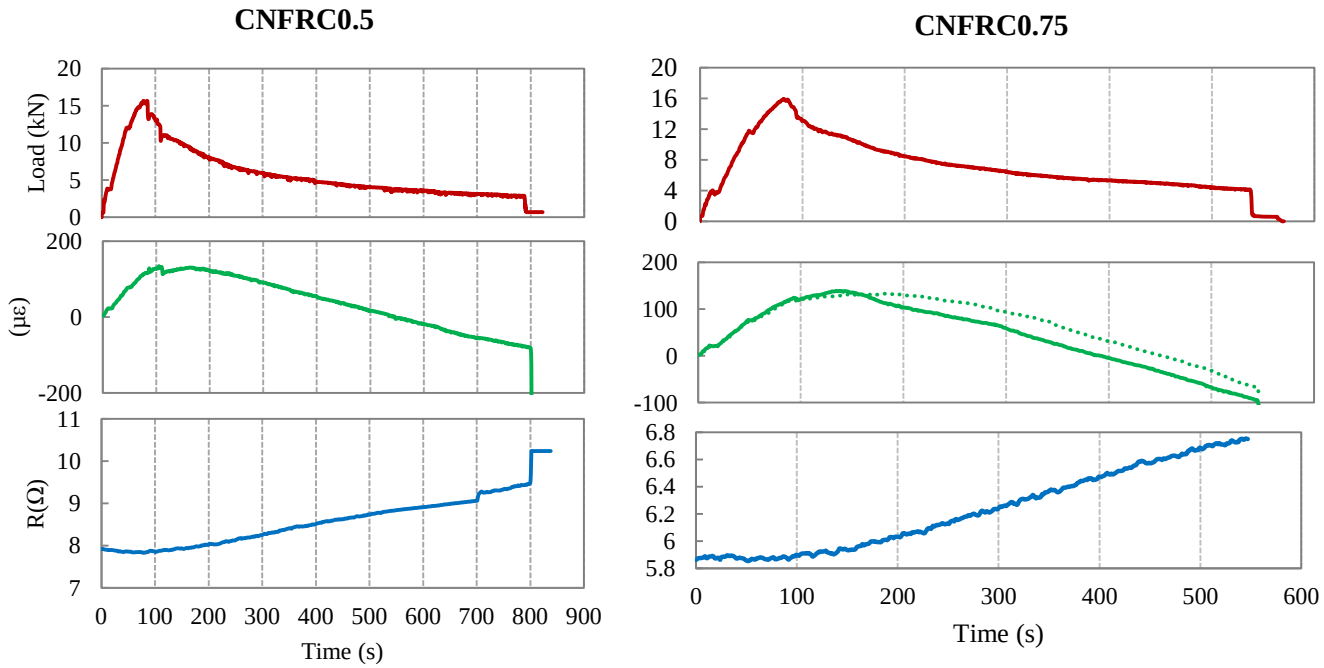

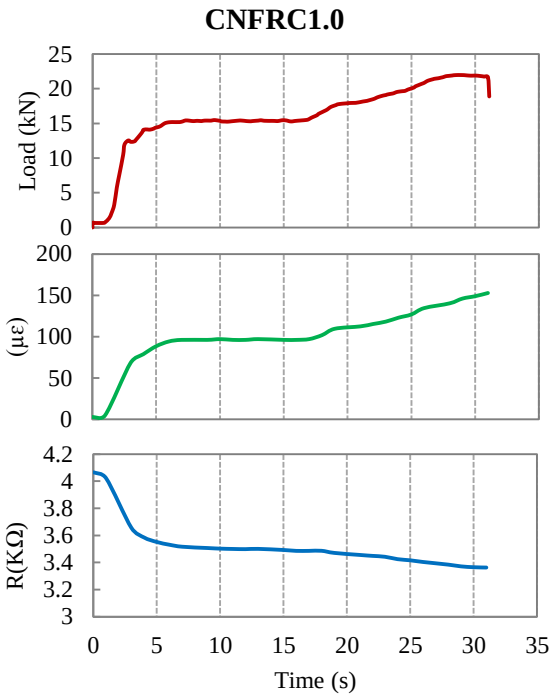

Figure 14: Time history results for CNFRC

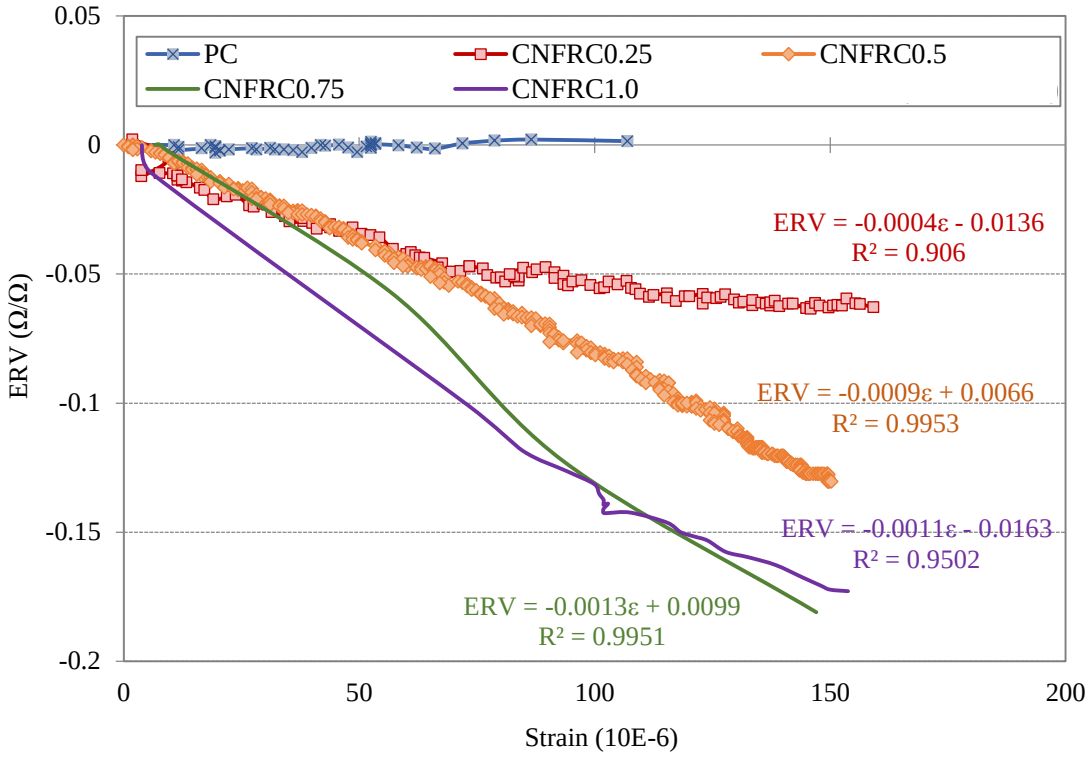

Figure 15: ERV vs. strain for all concrete types